Degradation of α-terpineol in aqueous solution by UV/H$_2$O$_2$: kinetics, transformation products and pathways

Jie Yao, Jinglin Guo, Zhaoguang Yang, Haipu Li and Bo Qiu

ABSTRACT

The monoterpene alcohol α-terpineol is extensively used as the foaming agent in mineral processing and can be released to environment along with the wastewater. This study evaluated the feasibility of eliminating α-terpineol in water by ultraviolet irradiation (UV) in combination with hydrogen peroxide (H$_2$O$_2$). Within an H$_2$O$_2$ dose of 10 mg/L and an UV fluence of 64.8 J/cm^2, more than 95% of the α-terpineol can be removed. The reactions fitted well to pseudo-first-order kinetics, and the apparent rate constant was 0.0678 min^{-1}. The effects of matrix species including various anions and humic acid (HA), were evaluated. The degradation rate decreased significantly with the addition of bicarbonate and HA. Further verification was carried out with three types of real water samples. In the ground water and the surface water, the degradation rate decreased likely due to the presence of natural organic matter. Finally, possible degradation pathways were proposed based on the identification of transformation products, and the occurrence of two main transformation products were monitored. This study demonstrated that the UV/H$_2$O$_2$ is an effective technology for the degradation of α-terpineol in water.

Key words | α-Terpineol, degradation, pathway, transformation product, UV/H$_2$O$_2$

Jie Yao
Jinglin Guo
Zhaoguang Yang
Haipu Li
Bo Qiu (corresponding author)
Center for Environment and Water Resources,
   College of Chemistry and Chemical Engineering,
Central South University,
Changsha 410083,
China
E-mail: qiubo1983@csu.edu.cn

Zhaoguang Yang
Haipu Li
Bo Qiu
Key Laboratory of Hunan Province for Water
   Environment and Agriculture Product Safety,
Changsha 410083,
China

INTRODUCTION

The monoterpene alcohol α-terpineol (see Figure 1) is widely used as a foaming agent in mineral processing due to its high surface activity and bubble size distribution (Brossard *et al.* 2005; Gupta *et al.* 2007; Vasseghian *et al.* 2014). It is also used as a fragrance in personal care products (Simonich *et al.* 2002). When released into the environment, it can lower water quality by depressing gas transfer at gas-liquid interfaces and increasing the solubility of other contaminants (Rosso *et al.* 2006). Moreover, it is considered as a precursor of disinfection by-products when it is discharged to drinking water sources. In August 2014, an illegal discharge of wastewater from the mineral processing plant to a drinking water source in Wushan, China, threatened the safety of drinking water for more than 50,000 people. In this accident, α-terpineol was found to be one of the main pollutants.

Previous research into the decomposition of α-terpineol has mainly focused on the gas phase or solid-gas interface as it is considered to be an indoor air pollutant (Wells 2005; Ham & Wells 2011; Shu & Morrison 2011). However, because α-terpineol can increase the stability of other pollutants in water as it is a surfactant, and because it can cause taste and odor complaints from customers if spilled into the water supply, studies on its degradation in water are also important. It is known that α-terpineol is stable in aquatic environments because of the ring structure and branched chains (Hou 2013), but it can be decomposed by soil bacteria (Tadasa 1977). Moreover, Hinrichs' group investigated multiphase ozonolysis of aqueous α-terpineol and found that the reaction products and kinetics differ from the gas-phase reaction (Leviss *et al.* 2016). In this paper, another advanced oxidation process (AOP) technique, UV/H$_2$O$_2$, is introduced for the treatment of α-terpineol in water.

UV/H$_2$O$_2$ is widely used in both wastewater and drinking water treatments due to its high treatment efficiency,
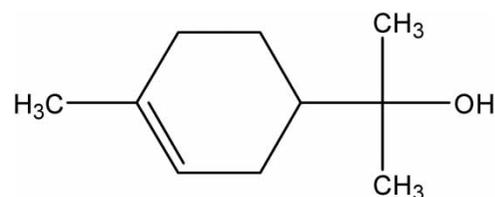

Figure 1 | Molecular structure of α-terpineol.

non-selectivity of the pollutants and resulting low concentration of disinfection byproducts (Canonica *et al.* 2008; Souissi *et al.* 2013; Tan *et al.* 2013; Aydin 2015; Carlson *et al.* 2015; Godayol *et al.* 2015). In the photodegradation process, H_2O_2 absorbs UV light and then generates highly reactive hydroxyl radicals (•OH), so the aqueous pollutants are decomposed by both UV direct photolysis and •OH-assisted indirect photolysis (Bolton & Cater 1994; Rosenfeldt *et al.* 2006).

The aims of this study were to investigate the removal efficiency of α-terpineol by UV/H_2O_2 treatment and to elucidate its transformation during the process. The effects of H_2O_2 concentration, pH, and matrix species on the degradation of α-terpineol were evaluated, and this treatment technology was also further examined and verified in different types of real water samples. Subsequently, transformation products in this degradation process were identified using gas chromatography-mass spectrometry (GC-MS), based on which two degradation pathways were proposed. Moreover, the changing trends of the two main transformation products were monitored.

MATERIALS AND METHODS

Materials and chemicals

The α-terpineol (90% technical grade) was purchased from Sigma-Aldrich (St. Louis, MO, USA). H_2O_2 (30% w/w), sodium chloride (99.5%), sodium sulfate (99.0%), sodium nitrate (99.0%), sodium bicarbonate (99.8%) and humic acid (90%) was purchased from Sinopharm Chemical Reagent Co., Ltd (Beijing, China). BSTFA (*N,O*-bis-trimethylsilyl-trifluoroacetamide) containing 1% TMCS (trimethylchlorosilane) was purchased from Sigma-Aldrich (St. Louis, MO, USA). PFBHA (*O*-(2,3,4,5,6-pentafluorobenzyl) hydroxylamine hydrochloride) and 4-acetylbutyric acid were purchased from TCI (Tokyo, Japan). Ethyl acetate and chloroform were purchased from Sigma-Aldrich (St. Louis, MO, USA) at GC-MS grade purity. Two standards of the transformation products, *p*-menthane-1,8-diol and 4-methylcyclohex-3-en-1-one were purchased from TCI (Tokyo, Japan) and Toronto Research Chemicals (Toronto, Canada), separately.

Photochemical reacting apparatus (BL-GHX-V, Shanghai) was used as the UV reactor. Ultrapure (UP) water (18.2 MΩ· cm, dissolved oxygen concentration (DOC) <0.1 mg/L) was obtained from a Persee (Beijing) pure water system. Prior to use, all glassware was cleaned with a laboratory detergent, rinsed with methanol and UP water, and baked in muffle furnace at 450 °C for 3 hours.

Photodegradation experiments

Photodegradation was conducted in a cylindrical glass reactor at room temperature. An 8 W low-pressure mercury lamp (Phillips) with the emission peak at 254 nm was placed coaxially with the reactor in a quartz sleeve, and the distance from the lamp to the reactor wall was 7.5 cm. The light intensity was determined as 18 mW/cm² at the lamp sleeve using a radiometer (Lutron YK-35UV). The molar absorption coefficients of α-terpineol and H_2O_2 at 254 nm were 43.8 L· mol^{-1}· cm^{-1} and 18.2 L· mol^{-1}·cm^{-1} respectively, measured by a UV/Vis spectrophotometer (TU-1901, Persee, China). The reactor was agitated by a magnetic stirrer operated at 300 rpm. The lamp was turned on 5 min before the experiment to ensure that the lamp was stable and had reached the full spectral output.

The initial concentration of α-terpineol was 20 mg/L and the initial concentrations of H_2O_2 were set at 5, 10, and 20 mg/L. Initial solution pH was adjusted with HCl or NaOH for the range of 2–12. Samples were withdrawn at preselected intervals, and each 1 mL of solution was extracted with 0.5 mL ethyl acetate after sampling. The extraction mixture was vortexed for about 30 seconds to ensure adequate contact between the water and the organic layer. The ethyl acetate layer was then analyzed with GC-MS. All experiments were conducted in triplicate.

Derivatization

Oximation and silylation were applied before GC-MS analysis to identify transformation products generated in the degradation procedure with carbonyl and hydroxyl/carboxyl groups, respectively. Three modes of derivatization strategies were used: oximation only, silylation only, and combined oximation and silylation. For oximation, 100 μL of PFBHA (0.05 mg/L) was added to the aqueous solution. Then the vials were left for 60 min to allow for the completion of the reaction. Silylation was performed after extraction with ethyl acetate. The organic layer was evaporated to dryness under a gentle stream of nitrogen. The residue was then treated with 100 μL of BSTFA + 1% TMCS and allowed to react at 65 °C for 90 min.

GC-MS analysis

GC-MS analysis was performed on an Agilent 7890A-5975C GC-MS (USA). A HP-5MS fused-silica capillary column (5% diphenyl/95% dimethyl-polysiloxane,

30 m × 0.25 mm × 0.25 μm, Agilent, USA) was used for separation. The GC temperature program was: initial temperature of 50 °C held for 2 min, followed by an increase of 20 °C/min to 105 °C, then increased by 5 °C/min to 115 °C, and finally increased by 20 °C/min to 240 °C and held for 0.5 min. The carrier gas was helium, with a constant flow of 1.0 mL/min. Splitless mode was used and 1 μL was injected. Electron impact with the electron energy of 70 eV was utilized. The m/z range was 50–500. The ion source temperature of the mass spectrometer was 230 °C. Quadrupole temperature and transfer line temperature were 150 °C and 280 °C, respectively.

RESULTS AND DISCUSSION

Effect of H$_2$O$_2$ concentration

Figure 2 shows the removal of α-terpineol versus time in the different experimental conditions tested. In the dark and with 10 mg/L of H$_2$O$_2$, no significant loss of α-terpineol was observed after 60 min, indicating the stability and persistence of the surfactant. The removal of the contaminant was significantly affected by UV irradiation and
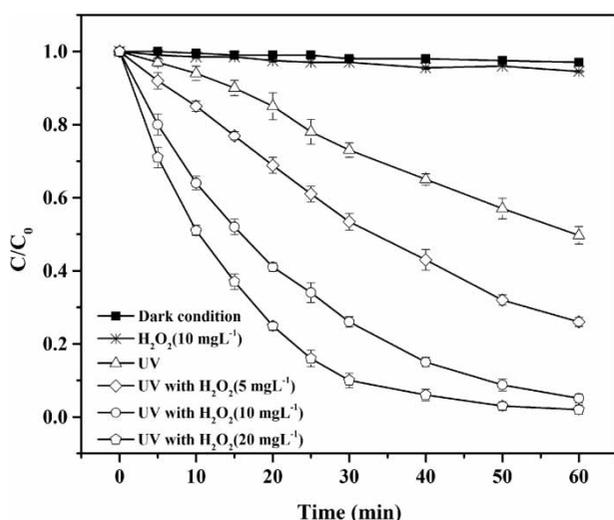
Figure 2 │ Removal of α-terpineol in darkness, H$_2$O$_2$ alone, UV irradiation alone and combined UV/ H$_2$O$_2$, respectively (Conditions: [α-terpineol]$_0$ = 20 mg/L, UV light intensity = 18 mW/cm^2, pH = 7).

UV/H$_2$O$_2$. When irradiated with UV only, the percentage removal was increased (approximately 50% in 60 min), and further acceleration was achieved by the addition of H$_2$O$_2$. The degradation of α-terpineol reached 74.2% within 60 min when 5 mg/L H$_2$O$_2$ was added. As the concentration of H$_2$O$_2$ increased to 10 mg/L and 20 mg/L, the degradation of α-terpineol reached 95.2% and 98.1% within 60 min, respectively. The results verified the importance of H$_2$O$_2$ in UV/H$_2$O$_2$ treatment for the generation of ·OH radicals to enhance the degradation of α-terpineol. In this system, H$_2$O$_2$ in solution acted as the electron acceptor, absorbed photons under UV irradiation, and produced ·OH radicals as a result of O-O bond ruptures. Free ·OH radicals could subsequently react with α-terpineol. With the increasing H$_2$O$_2$ concentration, the amount of ·OH radicals increased correspondingly (Keen *et al.* 2014), so the removal efficiencies of α-terpineol were increased.

The degradation reactions fitted well to the pseudo-first-order kinetics (see Table 1 for the coefficient of determination R^2 > 0.99) under UV irradiation without or with H$_2$O$_2$. The apparent rate constant K_{obs} increased from 0.0231 min^{-1} to 0.0678 min^{-1}, corresponding to the increase in H$_2$O$_2$ concentration from 5 mg/L to 20 mg/L. This was in agreement with the removal efficiencies observed. In the following experiments, the concentration of H$_2$O$_2$ was set to 10 mg/L due to the satisfactory degradation efficiency.

Effect of pH

In the photodegradation process, pH is a significant parameter because it can alter the charge state of the pollutants and influence the formation of active hydroxyl radicals (Chong *et al.* 2010; Lin *et al.* 2014; Kuo *et al.* 2015). In this study, as α-terpineol is a very weak acid (pKa = 15.09), it could remain in its undissociated form in the pH range investigated (2, 4, 7, 10, 12). Thus the change of the reaction rate at different pH values can be attributed to the generation of hydroxyl radicals. As

Table 1 │ Kinetic parameters of degradation of α-terpineol under UV irradiation and UV/H$_2$O$_2$ (Conditions: [α-terpineol]$_0$ = 20 mg/L, UV light intensity = 18 mW/cm^2, pH = 7)

Condition	Kinetic equation	Reaction rate constant K_{obs}/(min^{-1})	R^2
UV	ln(C$_0$/C) = 0.012t − 0.0458	0.012	0.990
UV + 5 mg/L H$_2$O$_2$	ln(C$_0$/C) = 0.023t − 0.0552	0.023	0.995
UV + 10 mg/L H$_2$O$_2$	ln(C$_0$/C) = 0.050t − 0.0705	0.050	0.997
UV + 20 mg/L H$_2$O$_2$	ln(C$_0$/C) = 0.068t + 0.0469	0.068	0.993

Table 2 │ Kinetic parameters of degradation of α-terpineol of different pH under UV/H₂O₂ (Conditions: [α-terpineol]$_0$ = 20 mg/L, [H₂O₂] = 10 mg/L, UV light intensity = 18 mW/cm²)

pH	Kinetic equation	Reaction rate constant K_{obs}/(min^{-1})	R^2
2	$\ln(C_0/C) = 0.0579t - 0.0683$	0.058	0.994
4	$\ln(C_0/C) = 0.0534t - 0.0571$	0.053	0.992
7	$\ln(C_0/C) = 0.0497t - 0.0705$	0.050	0.997
10	$\ln(C_0/C) = 0.0458t - 0.0172$	0.046	0.997
12	$\ln(C_0/C) = 0.0322t - 0.0659$	0.032	0.995

Table 2 shows, the degradation reactions fitted well to pseudo-first-order kinetics under acidic, circumneutral and alkaline conditions. The degradation rate decreased slowly when the initial pH increased from 2 to 10, which can be attributed to a higher redox potential of ·OH/H₂O in acidic conditions (Xiao *et al.* 2014). Moreover, the degradation rate decreased quite clearly when the pH increased from 10 to 12, probably due to (1) self-decay of H₂O₂ being enhanced under high pH conditions; (2) the fraction of hydroperoxide anion (HO₂⁻) becoming dominant with the increasing pH and acting as a strong ·OH scavenger (Tan *et al.* 2013). So if the pH of the wastewater was higher than 10, acidification would be necessary for a satisfactory degradation efficiency. However, this condition is not common.

Effect of matrix species

Further investigation was conducted to evaluate the effects of matrix species including chloride, nitrate, sulfate, bicarbonate and humic acid (HA) as they are commonly found in natural water systems as well as wastewater.

As Figure 3 shows, when sulfate or chloride was spiked into the reaction solution, the degradation kinetics remained the same as that obtained in the UP water solution. In contrast, the degradation rate decreased with the addition of 100 mg/L NO₃⁻. It can be rationalized that the UV absorption by nitrate was slightly higher than that of other anions at 254 nm (Xiao *et al.* 2014). Nitrite was also present in the solution (100 mg/L), and it is a powerful scavenger of hydroxyl radicals (Ward *et al.* 1996; Mack & Bolton 1999; Sharpless & Linden 2001). Although bicarbonate did not absorb UV light, a significant inhibitory effect was observed. It is known that bicarbonate is a radical scavenger in the AOP process, and can quench ·OH at a rate of 8.6×10^6 M^{-1}s^{-1} (Buxton *et al.* 1988; Liu *et al.* 2012), so
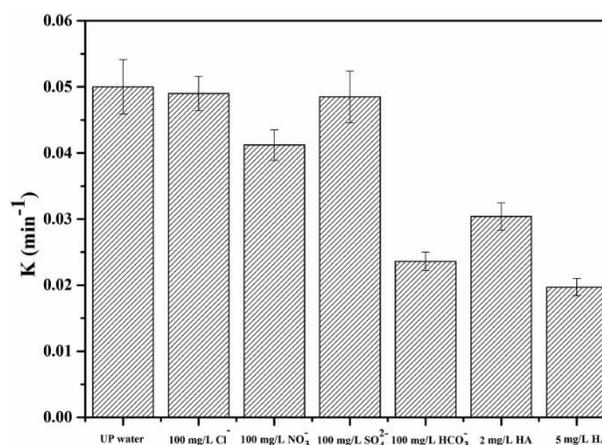
Figure 3 │ Effect of matrix species including Cl⁻, NO₃⁻, SO₄²⁻, HCO₃⁻, and HA on the photodegradation kinetics in UP water (Conditions: [α-terpineol]$_0$ = 20 mg/L, [H₂O₂] = 10 mg/L, UV light intensity = 18 mW/cm², pH = 7).

this result also demonstrated the important role of ·OH in UV/H₂O₂ treatment degradation of α-terpineol.

HA is often selected as a matrix species to investigate the effect of natural organic matter (NOM) on the degradation of contaminants in water (Prados-Joya *et al.* 2011). As shown in Figure 3, HA had an obvious negative effect on the degradation rate of α-terpineol. On the one hand, HA consists of a great number of aromatic rings and oxygen related functional groups leading to a competitive absorbance of photons. On the other hand, HA can act as a strong scavenger of ·OH (Crittenden *et al.* 1999). These two effects resulted in a significant inhibition of the degradation of α-terpineol in the presence of HA.

Photodegradation of α-terpineol in different types of water

To assess the degradation effectiveness of α-terpineol by UV/H₂O₂, experiments were carried out in real water samples, including groundwater (collected from Yuelu Mountain, Changsha), surface water (collected from Xiangjiang River, Changsha), and the effluent of a mineral processing plant (collected from Chenzhou City, Changsha). Here the nitrate concentration was detected by an ion chromatograph with electrical conductivity detector, the total alkalinity was analyzed by titration with hydrochloric acid, and the total organic carbon (TOC) was detected by a TOC analyzer (Shimadzu, TOC-V$_{CSH}$). It should be noted that the TOC values of groundwater and surface water were measured before 20 mg/L α-terpineol was spiked, while the concentration of α-terpineol in the effluent was 23 mg/L, contributing 73% of the TOC. No more α-terpineol was added to the effluent.

Table 3 | Effect of different types of water on degradation kinetics of α-terpineol (Conditions: [H$_2$O$_2$] = 10 mg/L, UV light intensity = 18 mW/cm^2, the spiked concentration of α-terpineol was 20 mg/L except for the effluent)

	UP water	Groundwater	Surface water	Effluent
pH	6.2	7.5	6.6	8.7
Nitrate (mg·L^{-1})	<0.05	2.20	3.52	7.41
Total alkalinity (as CaCO$_3$, mg·L^{-1})	<5	6	9	20
TOC (mg·L^{-1})	0.084	1.87	4.02	24.6
K$_{obs}$ (min^{-1})	0.050	0.046	0.035	0.036

As shown in Table 3, the pH values of the four water samples varied in a small range and the concentrations of nitrate and bicarbonate were all less than 20 mg/L, so according to the preceding discussion, the reduction of degradation rate in groundwater and surface water was mainly attributed to the NOM as they had higher TOC values than that of UP water. Interestingly, the TOC of the effluent was six times higher than that of the surface water, but the degradation rates in these two water samples were quite close. A possible explanation was that the TOC in the effluent was mainly contributed by the foaming agent (α-terpineol itself) and collecting agents (used to change the hydrophobicity of the minerals). In China, xanthate is the most widely used collecting agent, which decomposes very quickly under UV irradiation (Fu et al. 2016), so the high TOC value in the effluent did not mean high content of NOM.
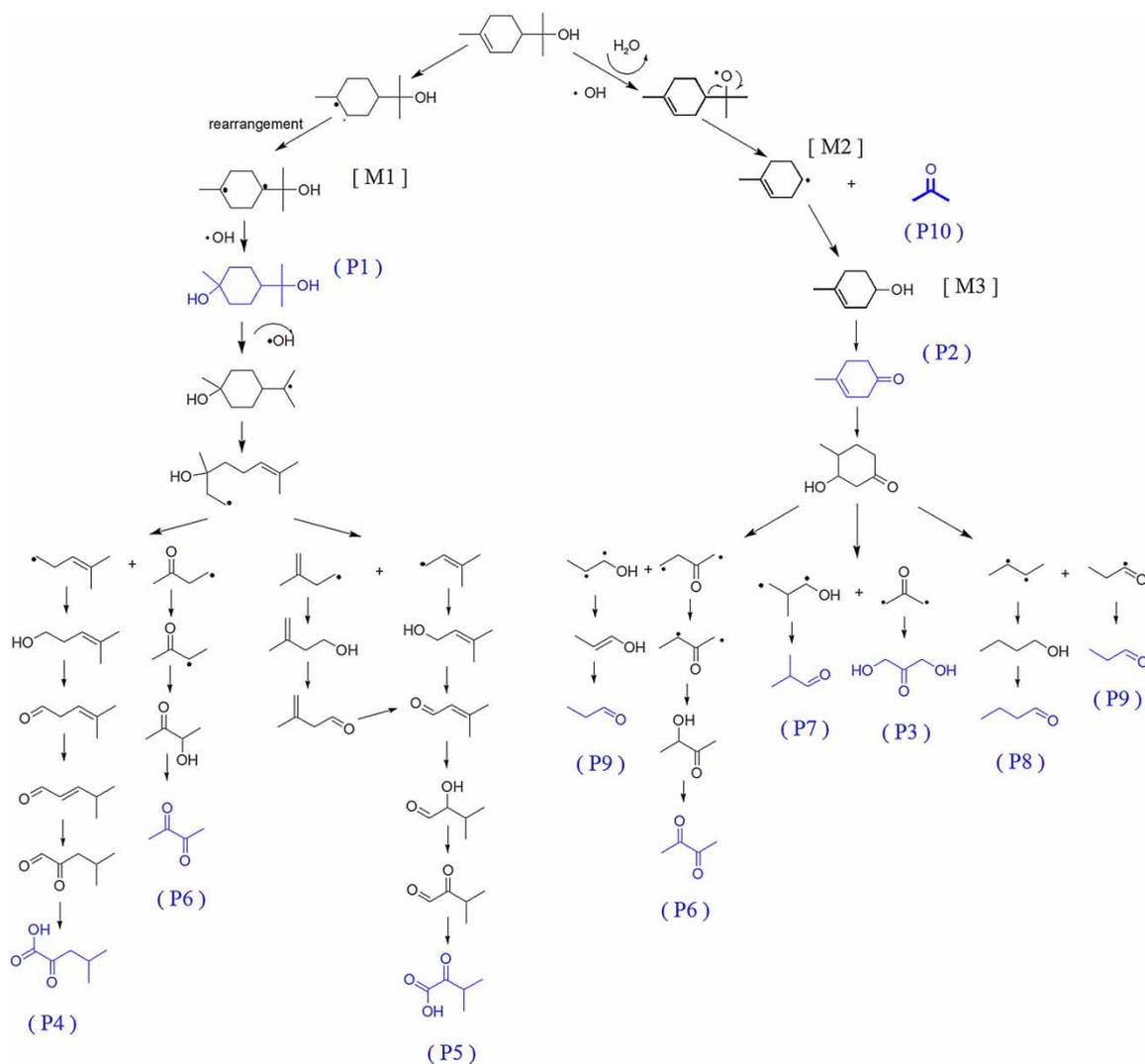
Figure 4 | Proposed degradation pathways of α-terpineol via identified transformation products with (a) GC-MS directly and (b) GC-MS after derivatization.

Identification of transformation products

In order to elucidate the possible degradation pathways of α-terpineol in UV/H$_2$O$_2$ treatment, the transformation products were identified by direct GC-MS and GC-MS after derivatization. The mass spectra were checked in the database from NIST MS Search 2.0 and compared with the GC-MS results of the degradation products of α-terpineol in the related references (Wells 2005; Ham & Wells 2008; Ham & Wells 2011). Ten transformation products (marked P1 to P10 in Figure 4 and Table 4) were found after UV/H$_2$O$_2$ degradation, among which P1 and P2 were much more abundant than the others identified. The mass spectra of their corresponding derivatives are presented in the Supplementary Material (see Figures S1–S10, available with the online version of this paper). It is important to note that the hydroxylated product (P1), which was confirmed by silylation experiments, has never been reported in the study of the degradation of gaseous α-terpineol

(Wells 2005; Ham & Wells 2008; Ham & Wells 2011), indicating an additional step in the degradation pathway of aqueous α-terpineol with an AOP system.

Proposed photodegradation pathways

Based on these identified products, two degradation pathways were proposed and illustrated in Figure 4. P1 and P2 were the two representative transformation products of the two degradation pathways, respectively. P1 suggested that the absorption of UV by the C-C bond initially led to the generation of the biradical, which rearranged to M1 (see Figure 4) due to the higher stability of the tertiary radical. One hydroxyl group was then added to the side chain, which had a lower steric hindrance, to form P1. P2, which was also found in the degradation of α-terpineol in the gas phase and at the gas-solid interface, suggested a different pathway, which started with the hydroxyl radical attacking
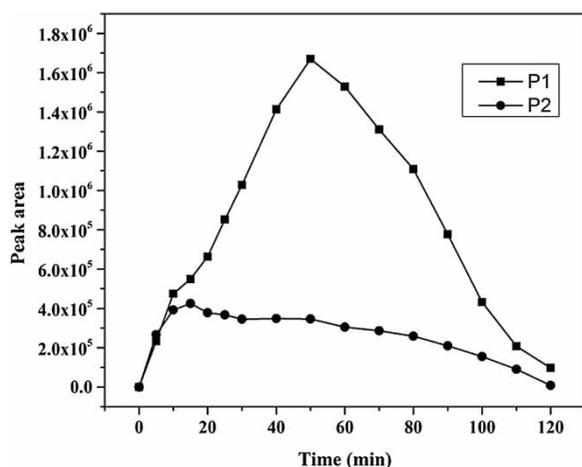
Table 4 | Molecular structure and confirmation methods of α-terpineol photodegradation transformation products

Product name	Molecular structure	Characteristic ions (m/z)	Identification method
p-Methane-1,8-diol (P1)		73, 81, 131, 211	Silylation
4-Methyl-3-cyclohexen-1-one (P2)		79, 107, 181, 288, 305	Oximation
1,3-Dihydroxyacetone (P3)		117, 161, 181, 195	Oximation
4-Methyl-2-oxopentanoic acid (P4)		73, 181, 200, 355, 382	Combined oximation and silylation
3-Methyl-2-oxobutanoic acid (P5)		73, 181, 366, 383	Combined oximation and silylation
2,3-Butanedione (P6)		181, 279, 476	Oximation
Isobutyraldehyde (P7)		56, 117, 181, 195, 250	Oximation
Butyraldehyde (P8)		161, 181, 195, 239	Oximation
Propionaldehyde (P9)		161, 181, 195, 236	Oximation
Acetone (P10)		72, 117, 181, 253	Oximation

the active hydrogen atom in the hydroxyl group of α-terpineol. After the production of P2, it underwent the cleavage of the C-C bond, hydroxylation of M2 and oxidation of M3 (see Figure 4). After the formation of P1 and P2, other small molecular weight products were generated via ring cleavage induced by hydroxyl radical attack or UV adsorption, combined with a series of rearrangements. The C-C bond cleavage by UV led to continual loss of carbon, and the hydroxylation-by-hydroxyl radical that followed generated smaller organic fragments containing aldehyde and carboxylic acid groups, such as the observed products (P3-P9) presented in the proposed pathways.

Occurrences of transformation products

P1 and P2 were two main transformation products, the concentrations of which were monitored in the UV/H$_2$O$_2$ process. As Figure 5 shows, the reactions generating P1 and P2 occurred in the initial stage of the photodegradation. The amounts of P1 reached a maximum at 50 min and progressively decreased in the following 70 min, whereas the amounts of P2 reached a maximum at 15 min and disappeared at 120 min. Considering that α-terpineol had degraded almost completely at 60 min when the H$_2$O$_2$ concentration was 10 mg/L and the initial concentration of α-terpineol was 20 mg/L (see Figure 2), P1 and P2 remained much longer than α-terpineol. It should be noted that although α-terpineol and P1 have low toxicity, P2 is suspected to be acutely toxic via the oral route and hazardous to the aquatic environment according to European Chemicals Agency (ECHA). So if a drinking water source was polluted by α-terpineol as in the accident in Wushan described above, particular attention should be paid to the occurrence of P2 in the relevant drinking water plants which apply UV/H$_2$O$_2$ as a disinfection technique.

CONCLUSIONS

This study demonstrated that UV/H$_2$O$_2$ is a promising technology for the degradation of α-terpineol in aqueous solution. With an H$_2$O$_2$ dose of 10 mg/L and a UV fluence of 64.8 J/cm^2 (light intensity: 18 mW/cm^2, irradiation time: 60 min), more than 95% of the α-terpineol can be removed. A high pH value was found to be negative to the degradation. The investigation into the matrix effects of Cl$^-$, HCO$_3^-$, NO$_3^-$, SO$_4^{2-}$ and HA suggested that the degradation could be significantly inhibited by HCO$_3^-$ and HA. Thus in the treatment of wastewater from mineral dressing plants, the water should be acidified and aerated to remove bicarbonate before photodegradation if bicarbonate or carbonate were applied in the flotation process.

Two possible degradation pathways were proposed based on the identification of the transformation products: the first one started from hydroxylation of the C-C bond and the second one began with cleavage of the side chain. Moreover, two main transformation products were monitored. They remained much longer under the UV/H$_2$O$_2$ treatment than α-terpineol, and one of them is suspected to be toxic. To break down this potentially toxic byproduct, nearly twice the UV fluence was required than to remove α-terpineol.

ACKNOWLEDGEMENTS

CONFLICT OF INTEREST STATEMENT

The authors declare no potential conflicts of interest.

Figure 5 │ The peak area vs. time profile of P1 and P2 on degradation of α-terpineol under UV/H$_2$O$_2$ (Conditions: [α-terpineol]$_0$ = 20 mg/L, [H$_2$O$_2$] = 10 mg/L, UV light intensity = 18 mW/cm^2, pH = 7).

REFERENCES

Aydin, E. 2015 Photolysis of naproxen under UV light: effect of natural organic matter and nitrate to transformation product formation. *Clean–Soil, Air, Water* **43** (1), 59–66.

Bolton, J. & Cater, S. 1994 Surface and Aquatic Environmental Photochemistry, Chapter 33, Boca Raton, FL: CRC Press, 467–490.

Brossard, L. E., Varela, N., Brossard, L. E., Brossard, C. O., Cortez, L. A. B. & Magalhaes, P. G. 2005 The surface-active bio oil solutions in sulfured copper mineral benefit. *Braz. J. Chem. Eng.* **22** (1), 1–7.

Buxton, G. V., Greenstock, C. L., Helman, W. P. & Ross, A. B. 1988 Critical review of rate constants for reactions of hydrated electrons, hydrogen atoms and hydroxyl radicals in aqueous solution. *Phys. Chem. Ref.* **17**, 513–886.

Canonica, S., Meunier, L. & von Gunten, U. 2008 Phototransformation of selected pharmaceuticals during UV treatment of drinking water. *Water Res.* **42** (1–2), 121–128.

Carlson, J. C., Stefan, M. I., Parnis, J. M. & Metcalfe, C. D. 2015 Direct UV photolysis of selected pharmaceuticals, personal care products and endocrine disruptors in aqueous solution. *Water Res.* **84**, 350–361.

Chong, M. N., Jin, B., Chow, C. W. & Saint, C. 2010 Recent developments in photocatalytic water treatment technology: a review. *Water Res.* **44** (10), 2997–3027.

Crittenden, J. C., Hu, S., Hand, D. W. & Green, S. A. 1999 A kinetic model for H$_2$O$_2$/UV process in a completely mixed batch reactor. *Water Res.* **33** (10), 2315–2328.

Fu, P., Feng, J., Yang, H. & Yang, T. 2016 Degradation of sodium n-butyl xanthate by vacuum UV-ozone (VUV/O3) in comparison with ozone and VUV photolysis. *Process Safe Environ.* **102**, 64–70.

Godayol, A., Gonzalez-Olmos, R., Sanchez, J. M. & Anticó, E. 2015 Assessment of the effect of UV and chlorination in the transformation of fragrances in aqueous samples. *Chemosphere* **125**, 25–32.

Gupta, A. K., Banerjee, P. K., Mishra, A., Satish, P. & Pradip. 2007 Effect of alcohol and polyglycol ether frothers on foam stability, bubble size and coal flotation. *Int. J. Miner Process* **82** (3), 126–137.

Ham, J. & Wells, J. 2008 Surface chemistry reactions of α-terpineol [(R)-2-(4-methyl-3-cyclohexenyl) isopropanol] with ozone and air on a glass and a vinyl tile. *Indoor Air* **18** (5), 394–407.

Ham, J. E. & Wells, J. R. 2011 Surface chemistry of a pine-oil cleaner and other terpene mixtures with ozone on vinyl flooring tiles. *Chemosphere* **83** (3), 327–333.

Hou, S. X. 2013 Determination the component of foaming agent and its natural degradation characteristics. *Adv. Mater. Res.* Trans Tech Publ, **641-642**, 351–354.

Keen, O. S., Ferrer, I., Michael Thurman, E. & Linden, K. G. 2014 Degradation pathways of lamotrigine under advanced treatment by direct UV photolysis, hydroxyl radicals, and ozone. *Chemosphere* **117**, 316–323.

Kuo, C. S., Lin, C. F. & Hong, P. K. 2015 Photocatalytic degradation of methamphetamine by UV/TiO$_2$ - kinetics, intermediates, and products. *Water Res.* **74**, 1–9.

Leviss, D. H., Van Ry, D. A. & Hinrichs, R. Z. 2016 Multiphase ozonolysis of aqueous alpha-terpineol. *Environ. Sci. Technol.* **50** (21), 11698–11705.

Lin, A. Y.-C., Lee, W.-N. & Wang, X.-H. 2014 Ketamine and the metabolite norketamine: persistence and phototransformation toxicity in hospital wastewater and surface water. *Water Res.* **53**, 351–360.

Liu, X., Garoma, T., Chen, Z., Wang, L. & Wu, Y. 2012 SMX degradation by ozonation and UV radiation: a kinetic study. *Chemosphere* **87** (10), 1134–1140.

Mack, J. & Bolton, J. R. 1999 Photochemistry of nitrite and nitrate in aqueous solution: a review. *J. Photoch. Photobio. A* **128**, 1–13.

Prados-Joya, G., Sánchez-Polo, M., Rivera-Utrilla, J. & Ferro-Garcia, M. 2011 Photodegradation of the antibiotics nitroimidazoles in aqueous solution by ultraviolet radiation. *Water Res.* **45** (1), 393–403.

Rosenfeldt, E. J., Linden, K. G., Canonica, S. & Von Gunten, U. 2006 Comparison of the efficiency of •OH radical formation during ozonation and the advanced oxidation processes O$_3$/H$_2$O$_2$ and UV/H$_2$O$_2$. *Water Res.* **40** (20), 3695–3704.

Rosso, D., Huo, D. L. & Stenstrom, M. K. 2006 Effects of interfacial surfactant contamination on bubble gas transfer. *Chem. Eng. Sci.* **61** (16), 5500–5514.

Sharpless, C. M. & Linden, K. G. 2001 DV photolysis of nitrate: effects of natural organic matter and dissolved inorganic carbon and implications for UV water disinfection. *Environ. Sci. Technol.* **35** (14), 2949–2955.

Shu, S. & Morrison, G. C. 2011 Surface reaction rate and probability of ozone and alpha-terpineol on glass, polyvinyl chloride, and latex paint surfaces. *Environ. Sci. Technol.* **45** (10), 4285–4292.

Simonich, S. L., Federle, T. W., Eckhoff, W. S., Rottiers, A., Webb, S., Sabaliunas, D. & De Wolf, W. 2002 Removal of fragrance materials during US and European wastewater treatment. *Environ. Sci. Technol.* **36** (13), 2839–2847.

Souissi, Y., Bouchonnet, S., Bourcier, S., Kusk, K. O., Sablier, M. & Andersen, H. R. 2013 Identification and ecotoxicity of degradation products of chloroacetamide herbicides from UV-treatment of water. *Sci. Total Environ.* **458–460**, 527–534.

Tadasa, K. 1977 Intermediates in the bacterial degradation pathway of α-Terpineol. *Agr. Bio. Chem.* **41** (10), 2095–2096.

Tan, C., Gao, N., Deng, Y., Zhang, Y., Sui, M., Deng, J. & Zhou, S. 2013 Degradation of antipyrine by UV, UV/H$_2$O$_2$ and UV/PS. *J. Hazard Mater* **260**, 1008–1016.

Vasseghian, Y., Heidari, N., Ahmadi, M., Zahedi, G. & Mohsenipour, A. A. 2014 Simultaneous ash and sulfur removal from bitumen: experiments and neural network modeling. *Fuel Process Technol.* **125**, 79–85.

Ward, M. H., Mark, S. D., Cantor, K. P., Weisenburger, D. D., Correa-Villasenor, A. & Zahm, S. H. 1996 Drinking water nitrate and the risk of non-Hodgkin's lymphoma. *Epidemiology* **7** (5), 465–471.

Wells, J. 2005 Gas-phase chemistry of α-terpineol with ozone and OH radical: rate constants and products. *Environ. Sci. Technol.* **39** (18), 6937–6943.

Xiao, Y., Fan, R., Zhang, L., Yue, J., Webster, R. D. & Lim, T.-T. 2014 Photodegradation of iodinated trihalomethanes in aqueous solution by UV 254 irradiation. *Water Res.* **49**, 275–285.